How small droplets form in turbulent multiphase flows

How small droplets form in turbulent multiphase flows

M. Crialesi-Esposito[1], G. Boffetta[2], L. Brandt[3,4], S. Chibbaro[5], and S. Musacchio[2]
1 *DIEF, University of Modena and Reggio Emilia, 41125 Modena, Italy*
2 *Dipartimento di Fisica and INFN, Università degli Studi di Torino, via P. Giuria 1, 10125 Torino, Italy.*
3 *FLOW Centre, KTH Royal Institute of Technology, Stockholm, Sweden*
4 *Department of Energy and Process Engineering, Norwegian University of Science and Technology(NTNU), Trondheim, Norway*
5 *Université Paris-Saclay, CNRS, LISN, 91400 Orsay, France*

The formation of small droplets and bubbles in turbulent flows is a crucial process in geophysics and engineering, whose underlying physical mechanism remains a puzzle. In this letter, we address this problem by means of high-resolution numerical simulations, comparing a realistic multiphase configuration with a numerical experiment in which we attenuate the presence of strong velocity gradients either across the whole mixture or in the disperse phase only. Our results show unambiguously that the formation of small droplets is governed by the internal dynamics which occurs during the break-up of large drops and that the high vorticity and the extreme dissipation associated to these events are the consequence and not the cause of the breakup.

Introduction The dynamics of droplet and bubble breakup in turbulence is fundamental for several industrial [1] and environmental processes [2, 3]. Because of the complex turbulent environment, drops typically have a broad range of sizes. In several cases, the diameter of the smallest droplets/bubbles is of the utmost importance, as for the dissolution of air bubbles in the oceans [4] or the transport of oil droplets deep into the marine environment after spilling [3]. The main actors at play in such processes are turbulence and capillarity, with the balance between the two determining the minimum droplet diameter for breakup to occur, before capillarity can resist the turbulent pressure fluctuations causing fragmentation. This threshold size is called the Kolmogorov-Hinze (KH) scale [5, 6], and on dimensional considerations reads as:

$$d_{KH} \sim (\rho_c/\sigma)^{-3/5}\langle\varepsilon\rangle^{-2/5}, \tag{1}$$

where ρ_c is the density of the carrier phase, σ is the surface tension and $\langle\varepsilon\rangle$ is the domain averaged turbulent energy dissipation rate. The fragmentation dynamics for droplets larger than the KH scale is understood in terms of a local cascade *à la Kolmogorov* [7], for which experimental and numerical evidences have been presented [2, 8, 9]. A broad spectrum of sub-Hinze droplets with diameter smaller than d_{KH} is also found. Despite recent attempts to understand this regime [10–13], the origin/dynamics of these small droplets in turbulence and their interaction with the surrounding flow remain mostly unknown.

A key feature of the breakup process appears to be the presence of strong velocity gradients in proximity of regions with high interfacial curvature, which contributes to increasing the local vorticity and creates areas of high energy dissipation [9]. Two possible complementary mechanisms are thought to be at the origin of the sub-Hinze droplets: (i) the presence of local events of extreme turbulence which induce a local decrease of the KH scale and cause the droplet breakup; (ii) capillary dynamics, which leads to a pinch-off and eventually generates intense dissipative events.

In the favour of the second scenario, experiments on the fragmentation of a single drop have shown that the sub-Hinze dynamics is non-local in size [11, 12], suggesting that the turbulence strain produces small filaments, which eventually leads to pinch-off via fast capillary dynamics [14]. One numerical example is shown in Figure 1, where a droplet larger than the KH size is deformed by turbulence into a thin ligament which, by Rayleigh-Plateau instabilities, produces several small droplets. Non locality is evident since the size of the daughter droplet is related with the diameter of the ligament and not of the entire droplet. Within this scenario, large dissipation events are induced by the rupture of the interface at the origin of sub-Hinze structures.

On the other hand, recent works have pointed out that the presence of the interface increases the probability of large vorticity and dissipative regions [15], leading to a higher intermittency than single-phase turbulence [9, 12]. This evidence might support the first mechanism (i), meaning that intense vorticity external to the droplets is the main cause of the fragmentation and the formation of sub-Hinze inclusions. Thus far, no numerical or laboratory experiment has been able to settle this issue and the statistical relevance of the two possible scenarios in particular in a realistic configuration with many droplets.

In this Letter, we address this dilemma by means of high-resolution numerical simulations, in which we control the small scale dynamics by penalizing the vorticity field, something not possible in a laboratory experiment [16]. The idea comes directly from Equation (1). In a local sense, $d \sim \varepsilon^{-2/5}$, suggests that small droplets are linked to regions of high dissipation. Hence, artificially penalizing the regions with strong velocity gradients (where $\varepsilon \gg \langle\varepsilon\rangle$) should enable us to understand where and how sub-Hinze structures are formed. Thanks to this surgery of the turbulent flow, we are capable to

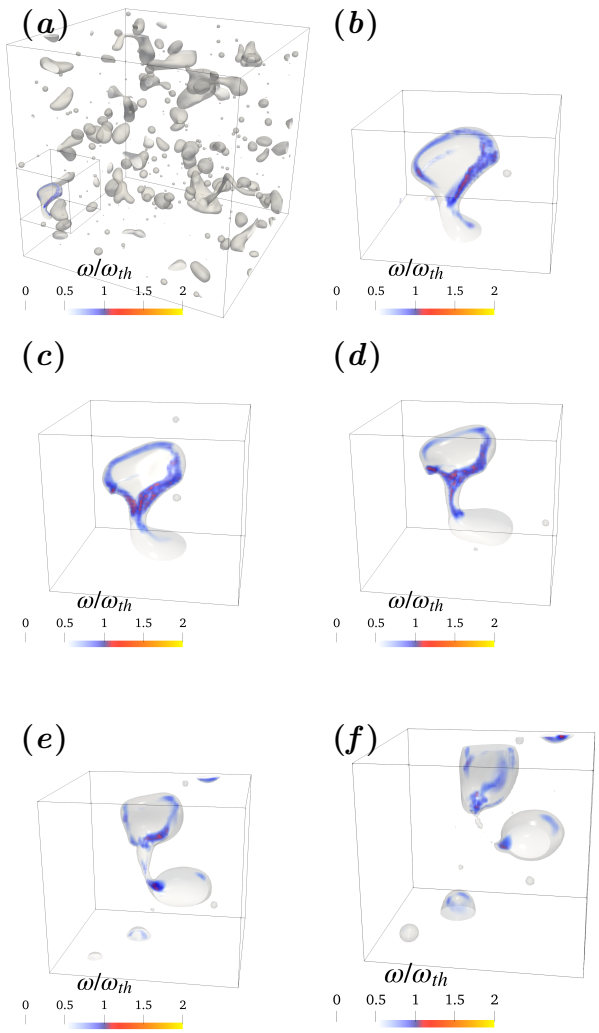

FIG. 1. Visualisation of high-intensity vorticity within the droplet during breakup. (a) a portion of the domain is extracted from the whole simulation. (b) beginning of a droplet breakup event: the droplet separates into two regions, divided by a neck; the vorticity inside the droplet shows high values ($\omega \approx \omega_{th}$) on the edges. (c-d) As the droplet deforms, regions of stronger vorticity form in proximity of the neck. (e-f) the breakup becomes inevitable and smaller droplets form as a result.

show that it is the flow *inside* the droplets which dominates the formation of very small droplets and the dynamics at the smallest scales, therefore supporting the second of the proposed mechanisms. Moreover, we show that turbulent extreme events have some impact on the structures with a diameter of the order of the KH scale, but are statistically negligible for the scales in the sub-Hinze range, where capillary effects are dominant. Our results demonstrate that the formation of small droplets below the KH scale is primarily dominated by capillarity, and, in turn, that the generation of small droplets is responsible for the presence of local maxima of vorticity and dissipation, rather than the contrary.

Methods We solve the one-fluid Navier-Stokes equations (NSE) including deformable interfaces [17]:

$$\frac{d\mathbf{u}}{dt} = -\nabla P + \nabla \cdot \left[\nu([\nabla \mathbf{u} + \nabla \mathbf{u}^{\mathrm{T}})\right] + \sigma \xi \delta_s \mathbf{n} + \mathbf{f} + \mathbf{f}^{\mathbf{C}}, \quad (2)$$

where $\mathbf{u}$ is the velocity field, P is the pressure, ν is the kinematic viscosity, ξ is the interface curvature, $\mathbf{n}$ is the interface normal, δ_s is a delta-Dirac function localised at the interface between the two phases, and σ is the surface tension coefficient. Turbulence is sustained through the ABC forcing $\mathbf{f}$ [18].

To control the flow we add the penalizing term $\mathbf{f}^C = -C\mathbf{u}$ [16], where regions of high vorticity ω can be suppressed directly in the momentum equation through the masking function:

$$C = \beta \left(\frac{tanh(\omega - \omega_{th}) + 1}{2} \right) , \quad (3)$$

where β is the filter amplitude ($\beta = 0$ corresponds to standard NSE), $\omega = |\sum_{ij}(\partial_i u_j - \partial_j u_i)|$ is the vorticity modulus, and $\omega_{th} = 5\sigma_\omega$ is the maximum threshold value, with σ_ω the standard deviation of the vorticity for the reference multiphase case (see below).

It is worth noticing that a penalization force which suppresses the regions with large values of the energy dissipation rate ε cannot be applied because its effect would be canceled by the pressure gradients. In a preliminary test, we observed that a direct masking based on ε alters the local structure of the velocity-gradient tensor and it does not preserve the incompressibility of the velocity field. Enforcing the incompressibility restores the local velocity gradients and cancels the effect of the penalization force. To overcome this issue we adopt a penalization method that suppresses the regions of high vorticity, which are linked to the events of strong dissipation while having a different local structure of the velocity gradients [19].

Simulations are carried out *via* the open-source code FLUTAS [20], and the interface is reconstructed using the Volume of Fluid method MTHINC [21]. Simulations are performed at the Taylor-scale Reynolds number $Re_\lambda = 137$, measured in the single-phase turbulent field [9]. The box-side length is 2π, discretised using $N = 512$ grid-points, with turbulence sustained at $L_f = \pi$, with a kinematic viscosity $\nu = 0.006$, and a matching density and viscosity between the phases. The volume fraction is $\alpha = V_d/V = 0.1$, where V_d is the volume of the dispersed phase and V is the volume of the computational domain. The large-scale Weber number is $We = \rho u_{rms}^2 L_f/\sigma = 42.6$. The present setup has been shown to develop a droplet distribution $N(d)$ displaying both the $-10/3$ and $-3/2$ scaling ranges at scales larger and smaller than the KH scale [9].

Numerical Results We report results from four numerical experiments, comparing three different multiphase simulations and one single-phase. Reference simulations are for single-phase (SP) and multiphase (MP)

flow. The two simulations in which the vorticity is penalized in the whole domain (MPp) and only inside the dispersed phase (MPp,i). For the results corresponding to the single-phase penalized simulation see Supplemental Material.

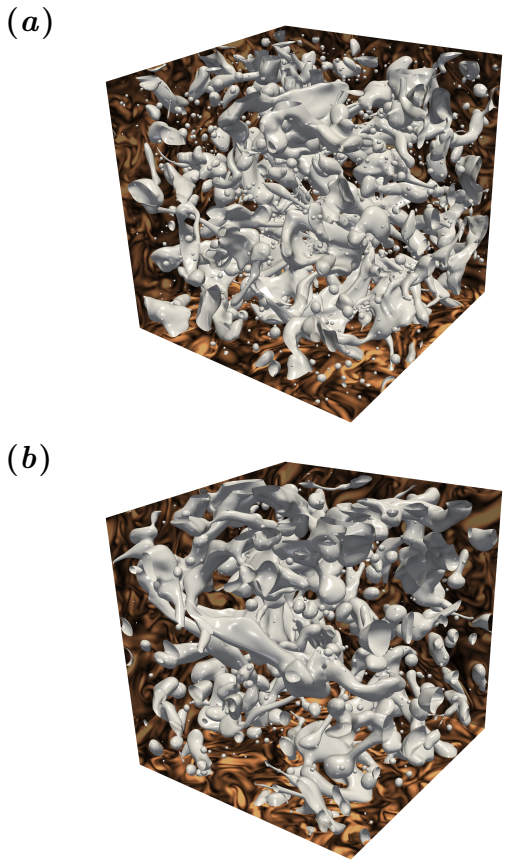

FIG. 2. Render of (a) non filtered MP flow and (b) filtered MPp flow. We show iso-contours of the color function (the droplet interface) and the vorticity field projected on the background planes.

From the visual comparison of the MP and MPp simulations shown in Figure 2, we may already qualitatively observe that suppressing local gradients partially inhibits the formation of small droplets, while preserving the large-scale flow structures. In particular, in the multiphase simulation with the penalization force (MP, Figure 2(b) we observe the formation of elongated fluid structures stretched by large-scale vortices, but the fragmentation of the droplets is overall attenuated.

To quantify the penalization effects, we report in Figure 3 the probability density function (PDF) of the vorticity magnitude (panel (a)) and of the energy dissipation (panel (b)). Comparing with the SP case, the MP flow displays an increment of the PDF tails both for vorticity and dissipation, confirming that the presence of the interface increases intermittency [12]. The increase is substantial for the energy dissipation. The effect of the filter appears in the vorticity PDFs sharply at $\omega = \omega_{th}$, i.e. exactly at the masking threshold. High values of ω are still possible due to the incompressibility constraint of Equation (2), as observed also for Navier-Stokes, SP simulations [16]. From Figure 3a it is evident that the statistics of vorticity obtained penalising inside the droplet phase only (MPp,i) is close to the unfiltered field MP, because of the penalization only acts on 10% of the total volume. The PDF of dissipation appears to be less affected by penalization. We find that the average dissipation in the MPp run is reduced of about 15% with respect to the MP case. According to Equation (1) this correspond to a change of 6% in d_{KH}.

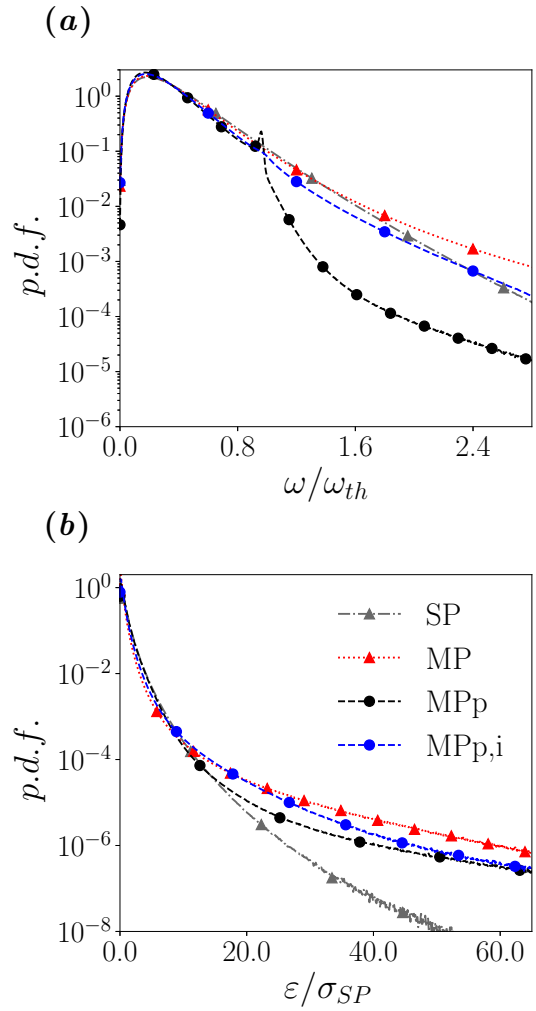

FIG. 3. Probability density functions of vorticity magnitude, panel (a) and energy dissipation $\varepsilon \equiv \nu|\partial_i u_j|^2$, panel ($b$). SP and MP refer to $C = 0$ cases, while MPp and MPp,i are the penalized cases, for which $\omega_{th} = 5\sigma_\omega$ (σ_ω being the vorticity standard deviation for case MP) and $\beta = 0.02$. Vorticity is normalised by ω_{th}, while energy dissipation by its standard deviation for the single-phase case σ_{SP}. The label i stands for inside, which indicates when the vorticity is penalised only inside the droplet phase, which corresponds to the $\alpha = 10\%$ of the mixture.

Further insight on the flow statistics is provided by the analysis of the PDF of the velocity increments $\delta_\ell u_\ell =$

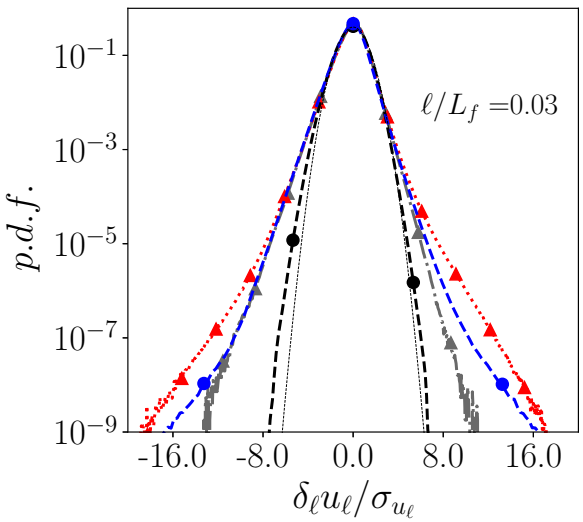

FIG. 4. PDF of velocity increments at $\ell = 0.03L_f$, normalized by the standard deviation for case SP. The PDF is obtained at small scales, much smaller than the Kolmogorov-Hinze scale. The legend is the same as in Figure 3.

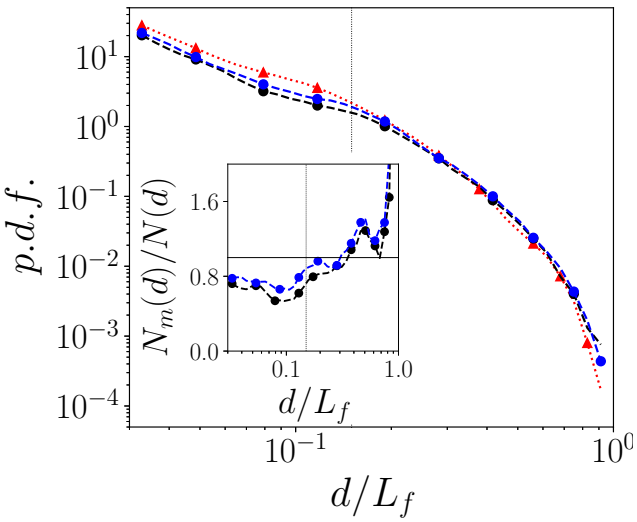

FIG. 5. Droplet-size-distribution for cases MP (red dotted line with triangles), MPp (black dashed line with dots), and MPp,i (blue dashed line with dots) where probability is obtained by normalizing all cases for the total number of droplets of the MP case. The inset shows the ratio for the total number of droplets of the filtered cases and the reference MP case. The black dotted vertical line represents the KH scale

$u(x+\ell) - u(x)$ [22], reported in Figure 4 for a separation below the Hinze scale. In the absence of penalization, the multiphase case (MP) is more intermittent, as also recently investigated [23]. When the mask is acting on the whole fluid (MPp case) the distributions become gaussian-like in multiphase flows, similarly to the single-phase case discussed in Ref. [16]. However, if the vorticity is filtered only inside the dispersed phase (MPp,i case) the probability distributions vary little when compared to the SP flow, the curves being distinguishable only in the far tails. This is explained by the low volume fraction considered, as most of the field (i.e. 90%) remains unchanged. The data lie between those of the the single phase and the multiphase flow, since the masking is not removing the interfaces, which are responsible for the increase in intermittency. Which scales are affected by the masking function is discussed in the Supplemental Material, where we show that penalizing strong vorticity regions is equivalent to act at scales below the Kolmogorov-Hinze one.

The effect of vorticity penalization (both in the dispersed phase and in the whole flow) on the droplet-size distribution is shown in Figure 5 together with the comparison with the unmasked case. To ease the comparison, we normalize the different curves by the total number of droplets of the unmasked MP flow. The distribution of large droplets (above the KH scale) for both the MPp and MPp,i cases are close to the MP reference run. However, significant quantitative differences are found in the total number of small droplets, especially for $d < d_{KH} \approx 0.15L_f$; notably, the number of droplets in the MPp flow is approximately 60% of those in the MP case. This can be better appreciated in the inset of Figure 5, where we display the ratio between the number of droplets of the masked cases and the unmasked MP case. As the mass is conserved, the number of larger droplets increases in the masked cases. The most important result is that the distribution is the same when the mask is applied to the whole mixture or only inside the dispersed phase. This observation is at odd with the statistics of dissipation which are almost unaffected by the penalization in the dispersed phase and demonstrates that high levels of vorticity and the most extreme dissipation events are a consequence of the destabilization process which leads to the breakup.

Discussion The present results indicate that the mechanism underlying the production of droplets below the Kolmogorov-Hinze scale in a turbulent emulsion is reduced when the vorticity is limited inside the droplets. Consequently, the origin of very small droplets can be traced back to capillary stresses, which act faster than the smallest turbulent eddies.

The following dynamical process has been unveiled: turbulent motions deform the droplets locally creating filaments, typically larger than the Kolmogorov-Hinze scale. Capillary instabilies are then triggered by the turbulent fluctuations (appearance of necks). This further reduces the filament dimension and produces vorticity inside the droplet, which, in turn, accelerates the filament instability in a self-sustained process, eventually leading to the rupture into different drops.

This last singular step is associated with strong vorticity release and increased dissipation. Therefore, extreme dissipation events are not the cause, but rather the effect of the break-up. Note also that the physics

of the fragmentation of droplets larger than d_{KH} is instead largely unaffected by the masking, confirming the quasi-local cascade *à la Kolmogorov* in this range.

Our findings show that it is possible to simplify the study of small droplets formation in turbulence by neglecting the action of large scale motion, and focusing on the droplet deformed state and its internal dynamics. For future works, it would be precious to analyse in detail the dynamics of the rupture of ligaments in relation with the creation of vorticity and dissipation. That would be important to build up reduced models relevant for applications.

Acknowledgments M.C.E. acknowledges the financial support given by the Department of Engineering 'Enzo Ferrari' of the University of Modena and Reggio Emilia through the action 'FAR dipartimentale 2023/2024'. S.M. and M.C.E. acknowledge EuroHPC for awarding access to MeluXina GPU through the project EHPC-REG-2022R01-052.

[1] D. J. McClements, *Food emulsions: principles, practices, and techniques* (CRC press, 2015).
[2] G. B. Deane and M. D. Stokes, Scale dependence of bubble creation mechanisms in breaking waves, Nature **418**, 839 (2002).
[3] M. Li and C. Garrett, The relationship between oil droplet size and upper ocean turbulence, Marine Pollution Bulletin **36**, 961 (1998).
[4] L. Deike, Mass Transfer at the Ocean–Atmosphere Interface: The Role of Wave Breaking, Droplets, and Bubbles, Annual Review of Fluid Mechanics **54**, 191 (2022).
[5] A. Kolmogorov, On the breakage of drops in a turbulent flow, Dokl. Akad. Navk. SSSR **66**, 825 (1949).
[6] J. O. Hinze, Fundamentals of the hydrodynamic mechanism of splitting in dispersion processes, AIChE Journal **1**, 289 (1955).
[7] C. Garrett, M. Li, and D. Farmer, The connection between bubble size spectra and energy dissipation rates in the upper ocean, Journal of Physical Oceanography **30**, 2163 (2000).
[8] A. Rivière, W. Mostert, S. Perrard, and L. Deike, Sub-hinze scale bubble production in turbulent bubble breakup, Journal of Fluid Mechanics **917**, A40 (2021).
[9] M. Crialesi-Esposito, M. E. Rosti, S. Chibbaro, and L. Brandt, Modulation of homogeneous and isotropic turbulence in emulsions, Journal of Fluid Mechanics **940**, A19 (2022).
[10] A. Rivière, D. J. Ruth, W. Mostert, L. Deike, and S. Perrard, Capillary driven fragmentation of large gas bubbles in turbulence, Physical Review Fluids **7**, 083602 (2022).
[11] Y. Qi, S. Tan, N. Corbitt, C. Urbanik, A. K. Salibindla, and R. Ni, Fragmentation in turbulence by small eddies, Nature Communications **13**, 1 (2022).
[12] M. Crialesi-Esposito, S. Chibbaro, and L. Brandt, The interaction of droplet dynamics and turbulence cascade, Communications Physics **6**, 5 (2023).
[13] A. Vela-Martín and M. Avila, Memoryless drop breakup in turbulence, Science Advances **8**, eabp9561 (2022).
[14] D. J. Ruth, W. Mostert, S. Perrard, and L. Deike, Bubble pinch-off in turbulence, Proceedings of the National Academy of Sciences **116**, 25412 (2019).
[15] D. Fuster and M. Rossi, Vortex-interface interactions in two-dimensional flows, International Journal of Multiphase Flow **143**, 103757 (2021).
[16] M. Buzzicotti, L. Biferale, and F. Toschi, Statistical properties of turbulence in the presence of a smart small-scale control, Physical Review Letters **124**, 084504 (2020).
[17] G. Tryggvason, R. Scardovelli, and S. Zaleski, *Direct numerical simulations of gas–liquid multiphase flows* (Cambridge university press, 2011).
[18] P. D. Mininni, A. Alexakis, and A. Pouquet, Large-scale flow effects, energy transfer, and self-similarity on turbulence, Physical Review E - Statistical, Nonlinear, and Soft Matter Physics **74**, 1 (2006).
[19] U. Frisch, *Turbulence* (Cambridge University Press, 1995).
[20] M. Crialesi-Esposito, N. Scapin, A. D. Demou, M. E. Rosti, P. Costa, F. Spiga, and L. Brandt, Flutas: A gpu-accelerated finite difference code for multiphase flows, Computer Physics Communications **284**, 108602 (2023).
[21] S. Ii, K. Sugiyama, S. Takeuchi, S. Takagi, Y. Matsumoto, and F. Xiao, An interface capturing method with a continuous function: The THINC method with multi-dimensional reconstruction, Journal of Computational Physics **231**, 2328 (2012).
[22] A. Monin and A. Yaglom, *Statistical fluid mechanics: mechanics of turbulence* (Courier Corporation, 2013).
[23] M. Crialesi-Esposito, G. Boffetta, L. Brandt, S. Chibbaro, and S. Musacchio, Intermittency in turbulent emulsions, Journal of Fluid Mechanics **972**, A37 (2023).